Available online at www.sciencedirect.com
ScienceDirect
Journal of Nuclear Materials 360 (2007) 293–303
journal of nuclear materials
www.elsevier.com/locate/jnucmat

Embrittlement susceptibility induced by impurities segregation to grain boundaries in martensitic steels candidates to be used in ADS

M. García-Mazarío *, A.M. Lancha, M. Hernández-Mayoral

CIEMAT, Avenida Complutense 22, 28040 Madrid, Spain

Received 3 January 2006; accepted 31 October 2006

Abstract

Grain boundary microchemical characterization, by Auger electron spectroscopy, has been performed in the martensitic steel EM-10 doped with relevant spallation elements that are expected to be produced at the spallation target window in future Accelerator Driven Systems (ADS). A heat treatment of step-cooling was performed in all doped materials to accelerate impurity segregation. The results indicate that step-cooling promotes chromium and molybdenum enrichment at the grain boundaries in the four materials studied. Step-cooling promotes phosphorus segregation to grain boundaries in the reference material, in the material doped with titanium, and in the material doped with titanium, phosphorus and sulphur. Step-cooling also promotes titanium enrichment in the materials doped with this element. A relation among chromium, molybdenum and phosphorus has been observed in the alloy doped with titanium, phosphorus and sulphur suggesting co-segregation of these elements to grain boundaries or segregation of phosphorus at the interface of the matrix and the carbides rich in chromium and molybdenum.

1. Introduction

An Accelerator Driven System (ADS) is a concept, which could allow transmutation of nuclear wastes with a good efficiency. Accelerator driven systems are one of the more suitable solutions together with the deep geological repository to get a more effective and with minimal potential risks management of nuclear wastes in a future at mid and long term.

One of the most important components for the viability of ADS is the spallation target. This target consists basically in the spallation material over which a high energy proton beam interacts, a window to separate the proton beam and the spallation material, the internals and the vessel. Due to the high energy of the incident proton beam, the irradiation conditions within the structure of the spallation target, in particular in the window, are expected to be severe and specific of this kind of systems. In the window, the direct impingement of the proton beam results in the production of spallation elements like hydrogen, helium, titanium, phosphorus, sulphur, calcium and vanadium. The production of these

* Corresponding author. Tel.: +34 91 3466616; fax: +34 91 3466661.
E-mail address: m.mazario@ciemat.es (M. García-Mazarío).

0022-3115/$ - see front matter © 2006 Elsevier B.V. All rights reserved.
doi:10.1016/j.jnucmat.2006.10.018

spallation elements will affect the microstructure and the microchemistry of the grain boundaries of the window materials. Hydrogen and helium can form bubbles and voids that will harden and embrittle the material; titanium and vanadium can precipitate producing hardening; titanium and calcium can form hydrides, which can produce embrittlement, and phosphorus and sulphur can segregate to grain boundaries and induce intergranular embrittlement or form sulphides and phosphides. In this work, the considered elements were phosphorus, sulphur and titanium. Both microscopical aspects, microstructure and microchemistry, are believed to influence macroscopical properties of the window materials and, consequently, they could affect the material behaviour under ADS operation. At present, 9–12Cr martensitic steels have been selected as prime candidates for the spallation target structures. However, the influence of the spallation elements on the behaviour of this type of martensitic steels is not known.

The aim of this work is to know the possible presence of relevant spallation elements at grain boundaries and to elucidate the effects that they could have on the behaviour of the materials candidate to be used in ADS systems. For this, studies of segregation to grain boundaries in the martensitic steel EM-10 doped with phosphorus and/or sulphur and/or titanium, with and without a special heat treatment of step-cooling to accelerate impurity segregation have been performed. In addition, undoped reference EM-10 steel with a heat treatment similar to the doped steels has been studied for comparison. The segregation studies have been performed by means of Auger Electron Spectroscopy (AES), which is one of the key techniques to study the grain boundary microchemistry in metals and alloys due to its inherent high depth resolution (~3 nm) and high spatial resolution (~50 nm). This work has been performed in the context of the SPIRE project of the 5th framework programme.

2. Experimental

2.1. Material

The materials studied are the following martensitic steels: EM-10 doped with titanium (EM-10Ti), EM-10 with low manganese and doped with sulphur (EM-10LMnS) and EM-10 doped with titanium, phosphorus and sulphur (EM-10TiPS). These steels have been compared with the reference EM-10R, that is the standard EM-10, but elaborated by the same way as the doped materials. The chemical composition and the heat treatments of the steels are shown in Table 1. These treatments, corresponding to the as-received condition, were applied with the aim to put in solid solution the doped elements and to obtain a material with a homogeneous matrix.

All materials were supplied by CEA, both in the as-received condition and after a step-cooling treatment. This treatment was applied to promote impurity segregation to grain boundaries. It consists in taking the material in the as-received condition (after the quench) and then perform an annealing with cooling the material in different steps from 650 °C to 520 °C during periods from 1 h to 72 h. During this heat treatment a precipitation of secondary phases is expected, but also segregation at boundaries of impurities and/or doping elements.

2.2. Sample preparation

In order to promote the intergranular fracture necessary to perform grain boundary segregation studies by AES, the preparation of the samples included a process of cathodic charging with hydrogen before the introduction and fracture of the samples inside the ultra high vacuum chamber of the Auger spectrometer. The cathodic charging with hydrogen was performed with the sample as cathode and an anode of platinum immersed in a solution 1 N of H_2SO_4, with the addition of As_2O_3 as a poison of recombination of hydrogen. The charging was performed at room temperature and the period of charging was approximately 72 h.

2.3. Auger Electron Spectroscopy (AES)

AES provides data on every element, except hydrogen and helium, present within the first 3 nm from the surface. The instrument used was a PHI 660 Scanning Auger Microprobe, which has a spatial resolution of approximately 50 nm. This system has a specially designed fracture stage attached to the spectrometer that allows to perform fracture by tension in ultra high vacuum, and also allows to analyse the two surfaces obtained after the fracture.

Table 1
Chemical composition (wt%) and heat treatments of the studied steels

	EM-10R	EM-10Ti	EM-10TiPS	EM-10LMnS
C	0.09	0.091	0.092	0.097
Ni	0.141	0.128	0.106	0.139
Cr	9.31	9.39	9.4	9.49
Mo	1.01	1.01	0.955	1
Cu	0.019	0.022	0.024	<0.01
Si	0.449	0.456	0.461	0.288
S	0.0005	0.0006	0.042	0.041
Al	<0.005	<0.005	<0.005	<0.005
Nb	0.005	<0.005	<0.005	<0.005
Co	0.016	0.015	0.016	0.0073
V	0.018	0.018	0.022	<0.005
Ti	0.008	0.209	0.238	0.0053
N	0.016	0.017	0.024	0.02
P	0.0054	0.0059	0.03	<0.003
Fe	Bal.	Bal.	Bal.	Bal.
Mn	0.403	0.434	0.435	<0.005
B	0.0011	0.0006	0.001	0.0009
W	<0.01	<0.01	<0.01	<0.01
Sn	0.003	0.0015	0.003	<0.0003
As	0.0036	0.0044	0.0034	<0.0003
Sb	0.0005	0.0005	0.0006	<0.0002
Heat treatment				
		1150 °C/30′ As-quenched		1200 °C/30′ As-quenched

After the cathodic charging with hydrogen, samples were fractured by tension at a deformation rate of 1 μm/s inside the Auger vacuum chamber, at a pressure of at least 2×10^{-9} Torr to minimise contamination. Spot analyses were performed on grain boundary facets and on ductile fracture for comparison. Spectra were collected using a beam energy of 10 keV and a target current of 0.3 μA, using these conditions the beam size is about 100 nm. The atomic concentrations were calculated according to Ref. [1]. Carbon and oxygen were not considered to calculate the atomic concentrations because their origin was mainly attributed to residual contamination from the vacuum chamber. Composition depth profiles were performed using a 2 keV argon ion flux, rastered over a 2×2 mm area, and with a pressure of argon of 5 mPa, yielding a sputter rate of about 3 nm/min calibrated with a Ta_2O_5 foil of known thickness.

This technique presents some difficulty to detect and quantify phosphorus in presence of molybdenum. These two elements have overlapping Auger electron transitions. The quantification of phosphorus in the cases, where molybdenum was present was done by using spectra of pure molybdenum, and subtracting the estimated peak-to-peak height of the molybdenum peak from the phosphorus signal.

3. Results

Two samples per each material condition were fractured and some intergranular fracture was obtained in all cases. As an example, Fig. 1 shows a detail of one of the obtained fracture surfaces.

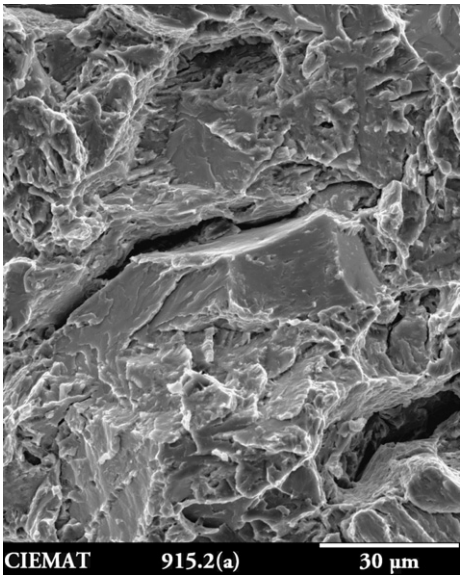

Fig. 1. Detail of a fracture surface.

3.1. EM-10R Steel

In the as-received condition the presence of the main elements of the alloy, iron and chromium, together with carbon and oxygen from residual contamination from the vacuum chamber were detected at ductile as well as at intergranular areas. After the step-cooling treatment a high percentage of intergranular areas showed, in addition, to the elements previously mentioned, phosphorus and molybdenum (Fig. 2).

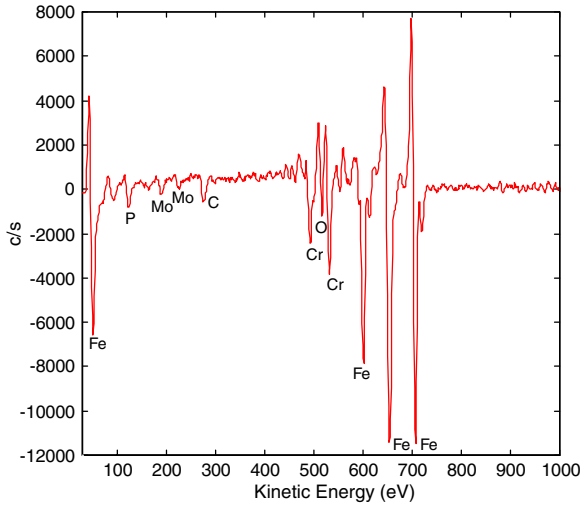

Fig. 2. Auger spectrum at an intergranular area of EM-10R step-cooled.

Quantitative results, Table 2, indicates no significant differences in the concentrations of chromium and iron at the ductile and intergranular areas in the as-received condition, while after step-cooling chromium enrichment and iron depletion at the intergranular areas can be observed (Fig. 3).

After step-cooling, depth composition profiles at intergranular areas indicated chromium enrichment and presence of phosphorus and molybdenum up to depths in the range from 3 nm to 20 nm (Fig. 4).

3.2. EM-10Ti Steel

In the as-received condition the spectra obtained at ductile areas were similar to those of the intergranular areas. Only in one intergranular area molybdenum was found. After the step-cooling treatment phosphorus, molybdenum and titanium were detected in some of the intergranular areas.

Quantitative results summarized in Table 2 indicates higher chromium concentrations and lower iron concentrations at the intergranular areas than at the ductile ones in the step-cooling material.

Depth composition profiles showed that chromium enrichment was present up to depths between 30 nm and 50 nm, phosphorus up to a maximum depth of 3 nm, molybdenum up to depths varying in the range from 6 nm to 60 nm, and titanium was detected up to depths between 3 nm and 10 nm. Fig. 5 shows a depth composition profile performed in one intergranular area, where an association

Table 2
Average concentration of Cr, Fe, P, Mo, Ti and S at ductile and intergranular areas in the studied materials (at.%)

			Cr	Fe	P	Mo	Ti	S
EM10R	As-received	Ductile	7 ± 2	93 ± 2	–	–	–	–
		Intergranular	9 ± 2	91 ± 2	–	–	–	–
	Step-cooling	Ductile	10 ± 2	90 ± 1	–	–	–	–
		Intergranular	14 ± 3	83 ± 5	1.2 ± 0.6	3.1 ± 0.8	–	–
EM10Ti	As-received	Ductile	7.0 ± 0.9	93.0 ± 0.9	–	–	–	–
		Intergranular	9 ± 2	90 ± 3	–	2.9	–	–
	Step-cooling	Ductile	11 ± 2	89 ± 2	–	–	–	–
		Intergranular	15 ± 5	81 ± 8	1.3 ± 0.6	5 ± 2	2 ± 1	
EM10LMnS	As-received	Ductile	9 ± 1	90 ± 1	–	–	–	2 ± 2
		Intergranular	12 ± 2	86 ± 3	0.9 ± 0.6	2.6 ± 0.9	–	2 ± 1
	Step-cooling	Ductile	10 ± 1	89 ± 2	–	–	–	2.4 ± 0.7
		Intergranular	19 ± 6	77 ± 8	0.5 ± 0.4	5 ± 2	–	1.8 ± 0.8
EM10TiPS	As-received	Ductile	10 ± 1	90 ± 1	–	–	–	–
		Intergranular	12 ± 2	86 ± 3	1.4 ± 0.4	2.8 ± 0.9	2.0	–
	Step-cooling	Ductile	10 ± 1	90 ± 1	–	–	–	–
		Intergranular	14 ± 4	78 ± 8	5 ± 1	4 ± 1	1.9 ± 0.7	–

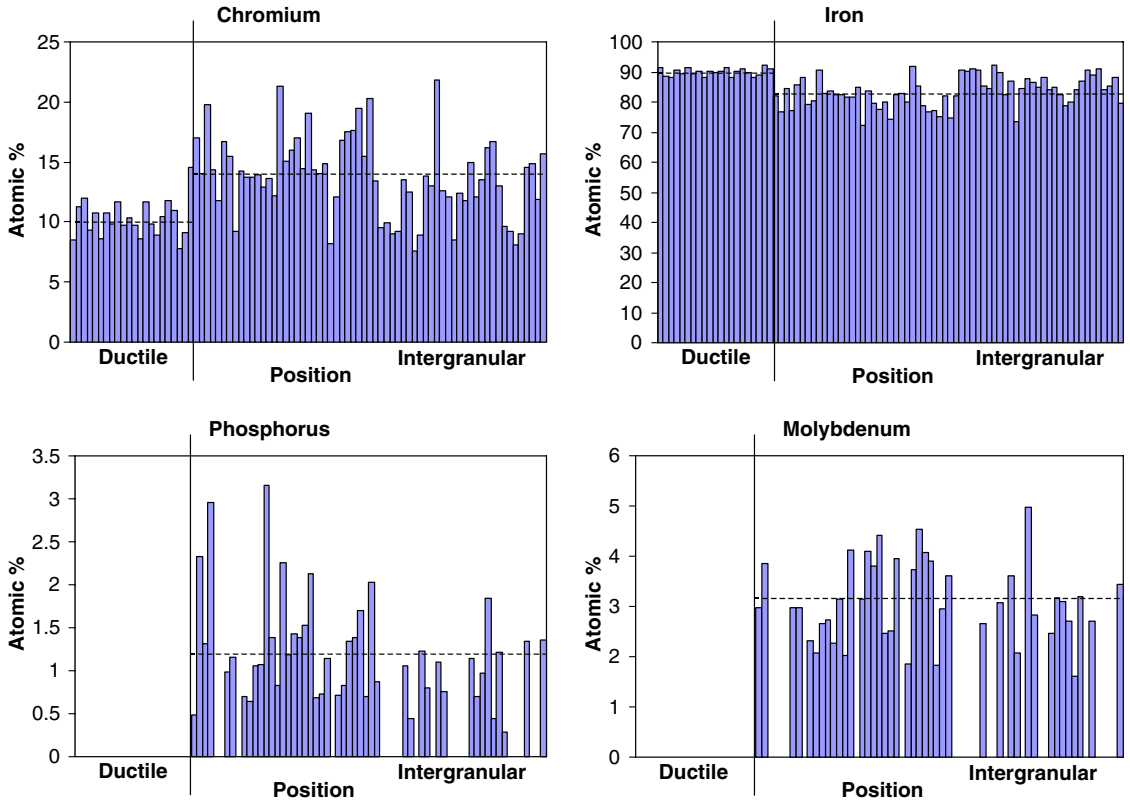

Fig. 3. Histograms of the fracture surface of EM-10R step-cooled.

between carbon, chromium and molybdenum can be observed from 0 to 30 nm suggesting the presence of carbides $M_{23}C_6$ type. In the outermost 5 nm, titanium could also be associated with the mentioned elements suggesting that it could be present as carbides, probably MC type. This relationship of carbon with chromium and molybdenum and titanium has not been observed in other cases.

3.3. EM-10LMnS Steel

Phosphorus, molybdenum and sulphur were detected in some of the intergranular areas of this material in the as-received condition as well as in the step-cooled material. Sulphur was also found in some of the ductile areas analysed.

In Table 2, clear chromium enrichment and iron depletion at intergranular areas can be observed in the step-cooled material. This chromium enrichment at intergranular areas was observed up to a depth between 50 nm and 70 nm. In addition, molybdenum was found up to depths lower than 3 nm in the as-received condition and between 3 nm and 30 nm after step-cooling, phosphorus was detected up to a maximum depth of 3 nm in both conditions and sulphur up to depths varying in the range from 3 nm to 90 nm in both conditions too. In some areas sulphur was seen associated to chromium (Fig. 6).

3.4. EM-10 TiPS Steel

In the as-received condition as well as after the step-cooling treatment, phosphorus, molybdenum and titanium were detected at intergranular areas, but the percentage of analyses, in which these elements were observed was clearly higher after the step-cooling treatment, Fig. 7 and Table 2.

In depth composition profiles in the as-received state phosphorus and molybdenum were detected up to depths lower than 3 nm. After step-cooling chromium enrichment was observed up to depths from 5 nm to 70 nm. Phosphorus was detected up to depths lower than 9 nm, molybdenum up to depths lower than 15 nm and titanium up to a maximum depth of 3 nm, Fig. 8.

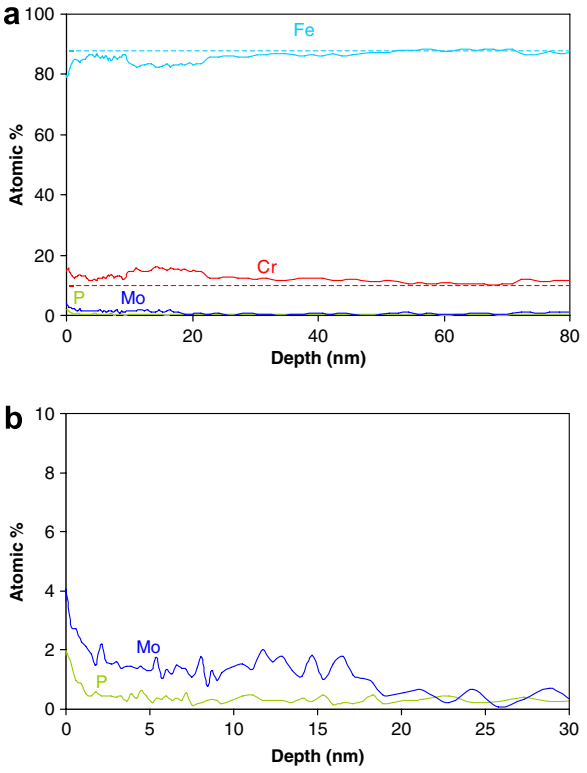

Fig. 4. Depth composition profile at the fracture surface of EM-10R step-cooled. (a) Intergranular area, (b) detail of (a).

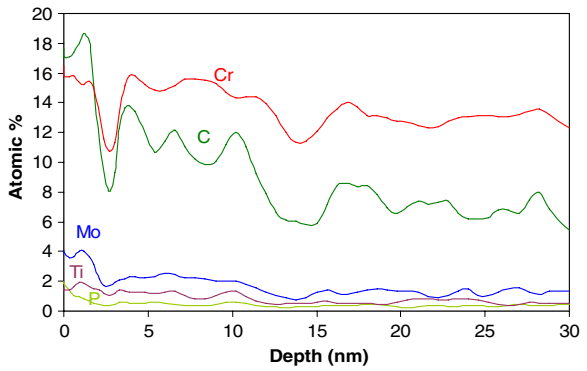

Fig. 5. Depth composition profile at the fracture surface of EM-10Ti step-cooled. Intergranular area. Fe, Cr, C, P, Mo and Ti normalized to 100%, but only Cr, C, P, Mo and Ti are represented.

4. Discussion

For a better comparison of the results corresponding to materials in the as-received condition and after step-cooling histograms of chromium, molybdenum, phosphorus and titanium, in which

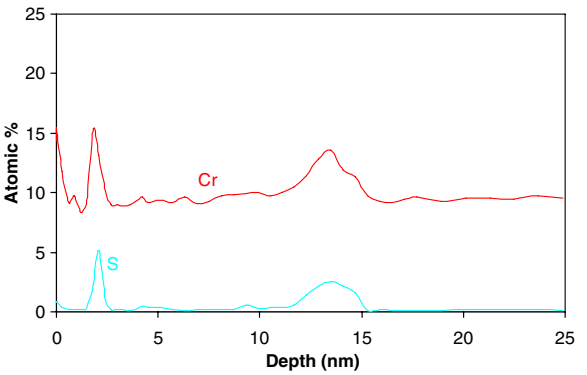

Fig. 6. Depth composition profile at the fracture surface of EM-10LMnS as-received. Intergranular area. Fe, Cr, S, Mo and P normalized to 100%, but only S and Cr are represented.

the frequency that these elements were detected at the intergranular areas with a determined concentration, were represented. Fig. 9 shows as an example the histograms for EM10TiPS.

Starting with chromium, in the four studied materials it can be observed that after step-cooling the distribution of chromium is shifted to higher chromium concentrations, therefore, step-cooling produces chromium enrichment. In the literature chromium enrichment has been reported in martensitic steels in the annealed and tempered condition and also in these materials with ageing heat treatments [2–10]. This chromium enrichment was attributed to segregation in some cases and to the presence of chromium carbides in other studies. In the present study the depth of chromium enrichment ranges from 3 nm to 70 nm. The depth of 3 nm suggests segregation of chromium, while the width of enrichment of 70 nm is in good agreement with the size of $M_{23}C_6$ carbides expected in this type of steel. In addition, in one of the depths profiles performed at intergranular areas, an association between chromium, carbon and molybdenum was seen. However, this relationship was not observed in other analysis. It is also possible that chromium enrichment exists at grain boundaries before the precipitation occurs. On the other hand, taking into account that the step-cooling treatment enhances segregation to grain boundaries and in the as-quenched studied materials also produces carbides precipitation, in the present work it is not possible to discard neither the possibility of chromium segregation nor the presence of carbides. Anyway, it has been reported that chromium at grain boundaries has a beneficial effect because it enhances the grain boundary cohesion [11].

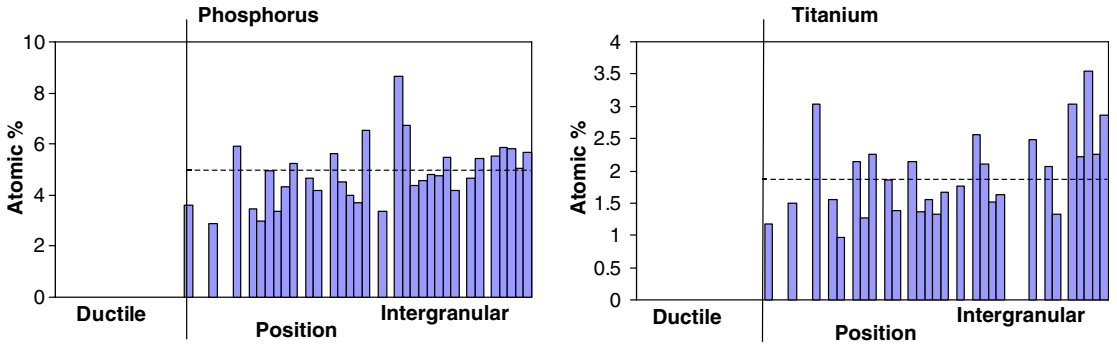

Fig. 7. Histograms of the fracture surface of EM-10 TiPS step-cooled.

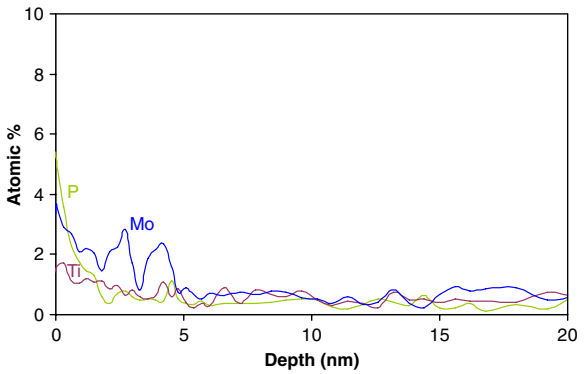

Fig. 8. Depth composition profile at the fracture surface of EM-10 TiPS step-cooled. Intergranular area. Cr, Fe, P, Mo and Ti normalized to 100%, but only P, Mo and Ti are represented.

Regarding molybdenum, in EM-10R step-cooling promotes the presence of molybdenum at grain boundaries that is not observed in the as-received condition. In EM-10Ti the situation is similar, in the as-received condition hardly exists molybdenum, while after step-cooling a high percentage of intergranular fracture shows molybdenum. In EM-10LMnS and EM-10TiPS an increase of the analysis percentage and concentration of molybdenum is also observed by effect of the step-cooling. Molybdenum was found up to depths from 3 nm to 60 nm. In a similar way to chromium, the depth of 3 nm suggest the presence of molybdenum segregated, while the depth of 60 nm indicates that this element is precipitated, thus, according to this depth molybdenum could be present in form of precipitate and/or segregated. It is known that molybdenum is an element that can be incorporated to the $M_{23}C_6$ carbides that are present at the grain boundaries. This fact seems to have been confirmed by some depth profiles performed in this work. Molybdenum enrichment at grain boundaries associated to the presence of carbides has been reported in martensitic steels [5]. On the other hand, as in the case of chromium, taking into account that step-cooling also enhances segregation, molybdenum could be segregated to grain boundaries. Molybdenum segregation to grain boundaries has also been reported in low alloy steels [12–15].

With respect to phosphorus, in the as-received condition this element was not detected in EM-10R and EM-10Ti. In these materials it is clearly observed that step-cooling produces segregation of phosphorus to grain boundaries. After step-cooling the EM-10LMnS steel shows an increase in the percentage of areas with phosphorus. In the as-received EM-10TiPS phosphorus was found in a high percentage of intergranular areas, most of the grain boundaries have phosphorus concentrations between 1 at.% and 2 at.%. After step-cooling a shift of the distribution of phosphorus to higher concentrations is clearly observed in this material, with most of the grain boundaries having phosphorus concentrations between 4 at.% and 6 at.%. Phosphorus was found up to a maximum depth of 18 nm indicating segregation. Therefore, step-cooling produces phosphorus segregation even in the materials not doped with phosphorus although, logically, the maximum segregation is produced in the material doped with this element. It has been reported phosphorus segregation in martensitic steels in the normalised and tempered condition and after ageing heat treatments [2–5,8,9,16].

As regards titanium, in EM-10Ti it has been detected after step-cooling only in ~10% of the intergranular areas analysed with a concentration around 2%. In EM-10TiPS this element was detected only in one area in the as-received condition and after step-cooling this element was detected in a great percentage of intergranular areas, most of

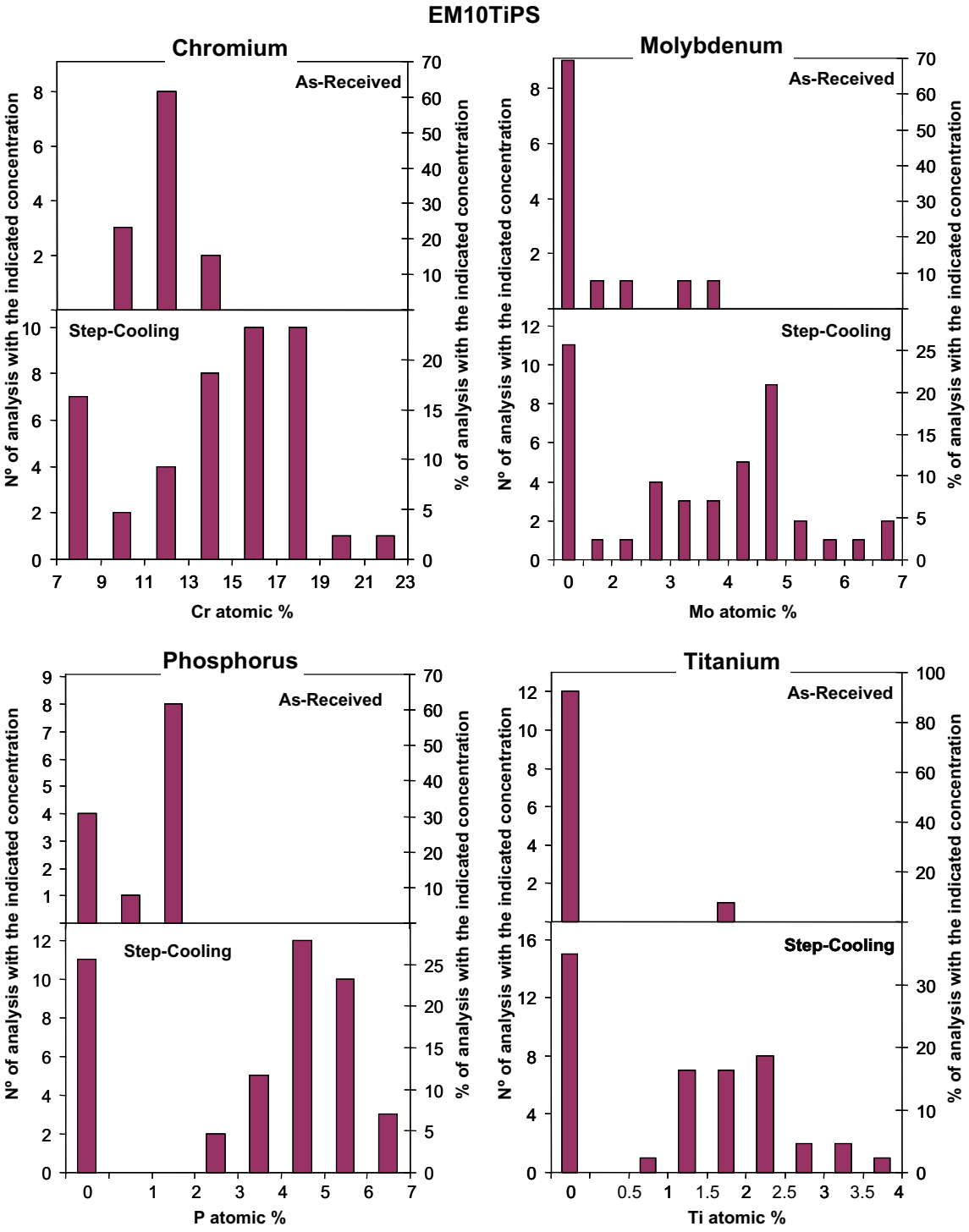

Fig. 9. Distributions of Cr, Mo, P, Ti at intergranular areas in EM10TiPS.

these areas showing values between 1% and 2.5%. Titanium was found up to depths lower than 9 nm indicating that is segregated or, more probably, precipitated as titanium carbides (MX particles) known to precipitate rapidly and with a smaller size compared to $M_{23}C_6$.

Table 3
Titanium and sulphur rich phases present in the doped steels [17]

	EM10Ti	EM10TiPS	EM10LMnS
Stable	TiN	TiN TiS–$Ti_4C_2S_2$ MnS	
Able to dissolve	Ti(Mo)C		CrS

According to CEA studies [17], Table 3 shows the stable and able to dissolve titanium and sulphur rich phases that can be present in these steels. The possibility of obtaining titanium and sulphur in solid solution, that may segregate after step-cooling, depends on the possibility of dissolving the phases rich in these elements during the high temperature heat treatment and to avoid their precipitation during cooling. CEA results showed that the normalization treatment at high temperature performed in these steels allowed to obtain some titanium in solid solution in matrix in the EM-10Ti steel, while for the EM-10TiPS steel the possibility of obtaining titanium in solid solution was very low. However, the Auger results suggest that in this material there was also some titanium in solid solution able to segregate or precipitate because after step-cooling clear enrichment of this element was detected. Titanium has been reported to enhance grain boundary cohesion [11].

In the sulphur doped steel (EM-10LMnS), sulphur segregation to grain boundaries has not been clearly observed because this element was observed at the intergranular areas as well as at the ductile ones. However, an association between sulphur and chromium has been detected in some depth profiles indicating the presence of CrS compounds in accordance with the CEA studies, Table 3. It is worth mentioning that these compounds are very narrow (<3 nm) and they have been detected easily by this technique.

The different elements observed at grain boundaries have been commented independently. Interactions of impurity elements with alloying elements, in particular interactions P–Cr–Mo have been mentioned in many papers due to the high interaction energy of complexes Cr–P and Mo–P [18].

With respect to the interaction Mo–P it has been reported [10] that in 12% Cr martensitic steels molybdenum has two opposite effects on phosphorus segregation. Molybdenum inhibits the segregation of phosphorus tying it up in the grain interior due to the strong Mo–P affinity and, on the other hand, molybdenum co-segregates with phosphorus counteracting the embrittlement effect of segregated phosphorus. The authors state that both beneficial effects of molybdenum are observed at intermediate nominal contents of this element (~0.7%). If the content in molybdenum increases to a critical value, precipitation of rich molybdenum carbides is produced and most of the molybdenum is removed from the solution giving free phosphorus to segregate. As regards the interaction Cr–P, in a similar way to the molybdenum, chromium has been reported to co-segregate with phosphorus at grain boundaries, but also it has been reported that at high concentrations chromium scavenges phosphorus in the matrix [8].

Other interpretation of the interactions Cr–P and Mo–P is that chromium and molybdenum enhance phosphorus segregation removing carbon, element that is known to compete with phosphorus by sites at grain boundaries, from the solution to form carbides [18]. Subsequent publications performed in low alloy steels indicate that the interactions Cr–P and Mo–P at grain boundaries as well as in the matrix are weak to influence in phosphorus segregation and consider more probable the interpretation that the relationship P–Cr–Mo is due to the interaction of the last two elements with carbon [12,19,20]. On the other hand, it has also been associated grain boundary phosphorus segregation to the existence of chromium carbides at grain boundaries. It has been reported that phosphorus segregates to the matrix–carbides interfaces [3,5,21].

In the present work, with the aim to know the possible existence of a relationship among chromium, molybdenum and phosphorus, graphs with the correlations Cr–Mo, Cr–P and Mo–P were represented. The case, in which a clear correlation among these elements was observed is in the EM-10TiPS steel (Fig. 10). The trend lines and the correlation factors seem to indicate that it exists a correlation Cr–Mo, a correlation P–Mo and a correlation P–Cr. These observations could be due either to co-segregation of phosphorus with chromium and molybdenum, or to segregation of phosphorus at the matrix–carbides interfaces.

Other elements that can interact are titanium and phosphorus. It has been reported that titanium scavenges phosphorus inhibiting the segregation of this element in low alloy steels [22]. This effect has not been observed in this study, the steels doped with titanium do not show a decrease in

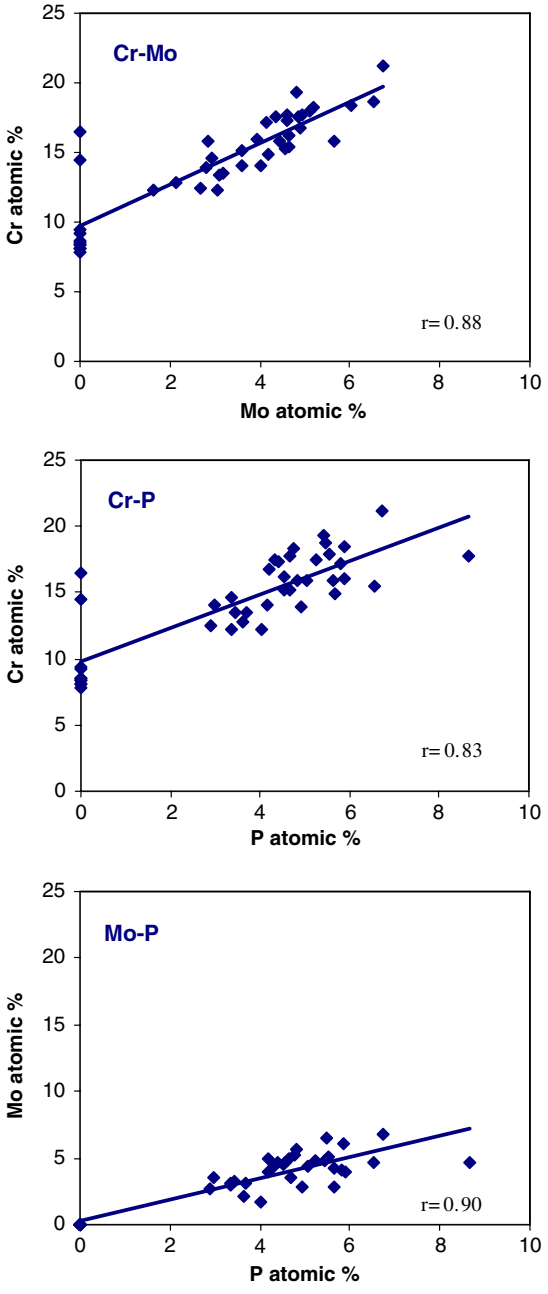

Fig. 10. Correlations Cr–Mo, Cr–P and Mo–P in the EM-10TiPS steel.

phosphorus segregation. Titanium also interacts with hydrogen. Titanium is a strong hydride former, and according to some authors it can co-segregate with hydrogen to form hydrides [11]. In the present study titanium has been observed at grain boundaries, but, unfortunately, hydrogen can not be detected by AES.

Finally, taken into account that the objective of this work is to study the existence of elements at grain boundaries that can be harmful in the materials candidates to be used in the ADS, it is worth mentioning that phosphorus segregation to grain boundaries has been observed even in the materials not doped with this element, and also in the conventional martensitic steels EM-10 and T-91 in the as-received condition [23]. This fact is important and it should be considered because phosphorus is known as an important embrittlement element to induce intergranular fracture. Other element that can result harmful is titanium. Titanium alone enhances grain boundary cohesion, but this beneficial effect is suppressed in the presence of hydrogen forming hydrides, which have a detrimental effect on the steel. Therefore, both phosphorus and titanium at grain boundaries could reduce the ductility of the martensitic steels under ADS operating conditions.

5. Summary and conclusions

- Grain boundary microchemical characterization has been performed in the steel EM-10 doped with relevant spallation elements (phosphorus, sulphur and titanium) with the aim to know the possible presence of these elements at grain boundaries and to elucidate the effects that this could have on the behaviour of the material. A special heat treatment of step-cooling was performed to accelerate impurity segregation to grain boundaries.
- Step-cooling produces chromium enrichment at grain boundaries in the four materials studied. Considering that the step-cooling treatment enhances segregation to grain boundaries and also produces carbides precipitation in the as-quenched studied materials, it is not possible to discard neither the possibility of chromium segregation nor the presence of chromium carbides.
- Step-cooling produces molybdenum enrichment in EM-10R and enhances molybdenum enrichment in EM-10Ti, EM-10LMnS and EM-10TiPS. As in the case of chromium, this enrichment could be attributed to segregation and/or the presence of molybdenum containing carbides.
- Step-cooling promotes phosphorus segregation to grain boundaries in EM-10R and EM-10Ti, and enhances phosphorus segregation in EM-10TiPS.

- A relation among chromium, molybdenum and phosphorus has been observed in EM-10TiPS steel suggesting co-segregation of these elements to grain boundaries or segregation of phosphorus at the matrix–carbides rich in chromium and molybdenum interface.
- Step-cooling promotes titanium enrichment to grain boundaries in EM-10Ti and enhances grain boundary titanium enrichment in EM-10TiPS. These results indicate that in both steels there is some titanium in solid solution able to segregate or precipitate.
- No clear segregation of sulphur to grain boundaries has been detected in the EM-10LMnS alloy before and after step-cooling.
- Phosphorus segregation at grain boundaries, even observed in undoped materials, is important and should be taken into account due to the well known embrittlement characteristics of this element for inducing intergranular fracture. Other element that can result harmful is titanium that can enhance grain boundary cohesion, but its beneficial effect is suppressed in presence of hydrogen forming hydrides, which have a detrimental effect on the steel. Therefore, both phosphorus and titanium at grain boundaries could reduce the ductility of the martensitic steels during the ADS operation.

References

[1] K.D. Childs, B.A. Carlson, L.A. LaVanier, J.F. Moulder, D.F. Paul, W.F. Stickle, D.G. Watson, Handbook of Auger Electron Spectroscopy, 3rd Ed., Physical Electronics, Eden Praire, MN, 1995.
[2] I.A. Vatter, J.M. Titchmarsh, Surf. Interface Anal. 25 (1997) 760.
[3] S. Mandziej, A.P. von Rosenstiel, H. Goretzki, M. Weiss, B.H. Kolster, Fresen. Z. Anal. Chem. 329 (1987) 335.
[4] M. Mackenbrock, H.J. Grabke, Mater. Sci. Technol. 8 (1992) 541.
[5] H. Goretzki, P.V. Rosenstiel, Spectrochim. Acta 40B (1985) 853.
[6] J. Lapeña, M. García-Mazarío, P. Fernández, A.M. Lancha, J. Nucl. Mater. 283–287 (2000) 662.
[7] P. Fernández, M. García-Mazarío, A.M. Lancha, J. Lapeña, J. Nucl. Mater. 329–333 (2004) 273.
[8] Ph. Lemblé, A. Pineau, J.L. Castagne, Ph. Dumoulin, M. Guttmann, Met. Sci. 13 (1979) 496.
[9] C.A. Hippsley, N.P. Haworth, Mater. Sci. Technol. 4 (1988) 791.
[10] R. Guillou, M. Guttmann, Ph. Dumoulin, Met. Sci. 15 (1981) 63.
[11] R. Gupta, Effect of spallation products on grain boundary cohesion, SPIRE Project, 5th framework programme, Contract FIKW-CT-2000-00058 (2004).
[12] P. Ševc, J. Janovec, M. Koutník, A. Výrostková, Acta Metall. Mater. 43 (1995) 251.
[13] J. Janovec, A. Výrostková, P. Ševc, J.S. Robinson, M. Svoboda, J. Krestanková, H.J. Grabke, Acta Mater. 51 (2003) 4025.
[14] A.J. Papworth, D.B. Knorr, D.B. Williams, Scripta Mater. 48 (2003) 1301.
[15] S.H. Song, Z.X. Yuan, D.D. Shen, J. Liu, L.Q. Weng, Mater. Sci. Technol. 20 (2004) 117.
[16] T. Angeliu, E.L. Hall, M.Larsen, A. Linsebigler, C. Mukira, in: Proceedings of the Conference on Advanced Heat Resistant Steels for Power Generation, San Sebastián, Spain, April 1998.
[17] O. Danylova, Y. de Carlan, D. Hamon, J.C. Brachet, J. Henry, A. Alamo, J. Phys. IV France 12 (2002).
[18] R.L. Klueh, D.R. Harries, High-chromium ferritic and martensitic steels for nuclear applications, ASTM stock number: MONO 3 (2001) ISBN 0-8031-2090-7.
[19] J. Perháčová, A. Výrostková, P. Ševc, J. Janovec, H.J. Grabke, Surf. Sci. 454–456 (2000) 642.
[20] C.J. McMahon Jr., Scripta Mater. 49 (2003) 1215.
[21] M. Hättestrand, M. Schwind, H.O. Andrén, in: Proceedings of the Conference on Advanced Heat Resistant Steels for Power Generation, San Sebastián, Spain, April 1998.
[22] P.E.J. Flewitt, R.K. Wild, Grain Boundaries their Microstructure and Chemistry, John Wiley, Chichester, England, 2001.
[23] M. García-Mazarío, A.M[a]. Lancha, SPIRE Project. Metallurgy before irradiation: Auger analysis on EM-10 and T-91 steels in the as-received condition, DFN/ME-12/IE-02, 2002.